Boosting the Performance of Zn Electrode in Aqueous Electrolytes via Trace Amount of Organic Molecules

Haiji Huang+,[a, b] Yan Wang+,[a] Dongmei Xie,[a] Jianyang Sun,[a] Jiachang Zhao,[a] Pinhua Rao,*[a] Won Mook Choi,*[b] and Jianfeng Mao*[c]

The poor performance of Zn electrode in aqueous electrolytes prevents the practical application of aqueous zinc-ion batteries (AZIBs). Here, 2-Pyrrolidinone (Pr) is introduced into conventional $ZnSO_4$ electrolytes as additive and only 3 vol.% addition (Pr-to-H_2O volume ratio) enables boosted performance. The Pr molecules are preferentially adsorbed on the surface of Zn electrodes to promote the uniform deposition of Zn ions and modulate the solvation structure of Zn^{2+} to inhibit the side reactions. As a result, the Zn electrode is boosted to run over 1200 h during charge/discharge cycling processes and delivers high average coulombic efficiency (CE) of 99.9% under $1\,mA\,cm^{-2}$, $1\,mAh\,cm^{-2}$. Even under harsh testing conditions of $20\,mA\,cm^{-2}$ and $20\,mAh\,cm^{-2}$, Zn electrode still run over 100 h, which is much longer than that at pristine electrolyte (25 h). Moreover, the Zn||MnO_2 full cells with the Pr additive exhibit a high capacity of $201\,mAh\,g^{-1}$ and good capacity retention of 89% after 550 cycles at $0.5\,A\,g^{-1}$.

Introduction

In recent years, achieving carbon neutrality to address the climate change calls the advanced energy storage technologies. Although lithium-ion batteries currently dominate the energy storage market, there are still challenges in cost and safety.[1,2] Aqueous Zn-ion batteries (AZIBs) have gaining strong attention due to the high theoretical capacity ($5851\,mAh\,cm^{-3}$ and $820\,mAh\,g^{-1}$) and low redox potential ($-0.76\,V$ versus the standard hydrogen electrode) of Zn metal anode and high safety of aqueous electrolyte.[3–5] In particular, AZIBs are promising for grid-scale storage. However, due to the strong activity of water, a series of side reactions such as hydrogen evolution reaction (HER), corrosion and Zn dendrite growth occur at the electrolyte/electrode interface. These issues lead to poor cycling stability of Zn electrodes and short-circuiting of batteries, limiting commercial applications.[6–10]

Several strategies have been attempted to promote the charge/discharge performance of Zn anode, including modification of Zn electrode and electrolyte engineering.[11–15] The structural modification of the Zn electrode surface is mainly achieved by a coating technology, which is however more time-consuming and labour-intensive.[11] Electrolyte engineering strategies include "water in salt" electrolytes,[12] hydrated deep eutectic electrolyte[13] and additives.[16] "Water in salt" electrolytes expand the window of electrochemical stability and reduce water activity. Hydrated deep eutectic electrolytes modulate the solvation structure of Zn^{2+}. However, the drawbacks of these methods are low ionic conductivity, high viscosity and high cost. In comparison, electrolyte additive is a practically promising approach because it is convenient and inexpensive.[16–25] However, the cycling stability of AZIBs remains practically difficult especially under harsh conditions of high capacity/current density of $>5\,mAh\,cm^{-2}$ and $5\,mA\,cm^{-2}$. It is known that the electrochemical performance of Zn metal anode is largely dependent on the physiochemical properties of the electrolyte and the Zn metal/electrolyte interface. Therefore, it is necessary to explore a suitable electrolyte additive that simultaneously manipulates Zn^{2+} solvation structure and regulates electrode–electrolyte interface to boost the stability of the Zn anode under harsh test conditions.

Here, we report the application of 2-Pyrrolidinone (Pr) molecules as an additive to the conventional $ZnSO_4$ electrolyte (2 M). The addition of Pr at 3 vol.% in the electrolyte (2MP3) significantly boosted the cycling stability and reversibility of the Zn anode. The experimental investigations and theoretical calculations demonstrated that the Pr molecule has strong coordination capability to regulate the solvation structure and inhibit the side reactions. Moreover, Pr molecules preferentially adsorb at the Zn metal surface, which balances the ion concentration and electric field distribution at the Zn electrodes, and achieves uniform Zn deposition. Importantly, the

[a] Dr. H. Huang,+ Y. Wang,+ D. Xie, J. Sun, Prof. J. Zhao, Prof. P. Rao
College of Chemistry and Chemical Engineering, Shanghai University of Engineering Science, Shanghai 201620, P. R. China
E-mail: raopinhua@sues.edu.cn

[b] Dr. H. Huang,+ Prof. W. Mook Choi
School of Chemical Engineering, University of Ulsan, 93 Daehak-ro Nam-gu, Ulsan, 44610 Republic of Korea
E-mail: wmchoi98@ulsan.ac.kr

[c] Dr. J. Mao
School of Chemical Engineering, The University of Adelaide, Adelaide, SA, 5005 Australia
E-mail: jianfeng.mao@adelaide.edu.au

[+] These authors contribute equally.

Batteries & Supercaps

Research Article
doi.org/10.1002/batt.202300526

Chemistry Europe
European Chemical
Societies Publishing

Zn–MnO$_2$ full cells with 2MP3 electrolyte exhibit superior cycling performance to pure ZnSO$_4$ electrolyte.

Results and Discussion

To investigate the effect of Pr electrolyte additive on the cycle stability of Zn electrodes, we compared the plating/stripping processes of Zn electrode in Zn∥Zn symmetrical cells containing ZnSO$_4$ electrolyte with and without Pr additive. The electrolyte system with 3% Pr (2MP3) additive exhibited best cycling stability among the electrolyte systems without and with different amount of Pr additives including 0 v/v% (2 M), 1 v/v% (2MP1), and 5 v/v% (2MP5) under different test condition, Figure 1a–c. Specifically, as shown in Figure 1a, the cell with pure ZnSO$_4$ (2 M) electrolyte showed inferior stable cycling performance for only 650 h at 1 mA cm^{-2}, 1 mAh cm^{-2}. In contrast, the Zn electrode has the longest lifespan of 1200 h in the 2MP3 electrolyte. Meanwhile, the cycle lifespan of Zn electrode decreased when Pr amount surpassed 3%. Even at 10 mA cm^{-2} and 10 mAh cm^{-2}, the Zn electrode in 2MP3 electrolyte can steadily cycle for 456 h, while the cell with 2 M electrolyte failed after only 70 h (Figure 1b). Significantly, the Zn electrode in 2MP3 electrolyte showed over 100 h cycling stability under harsh test conditions of 20 mA cm^{-2},

20 mAh cm^{-2} (Figure 1c), while the cells with 2 M electrolyte had a short circuit after 25 h. These results demonstrate the positive effect of 3% Pr additive on the cyclic stability and reversibility of Zn electrodes.

The Coulombic efficiency (CE) is an essential factor in evaluating the reversibility of Zn electrodes characterized by Zn∥Cu asymmetrical cells. As depicted in Figure 2a, the half cell in 2 M electrolyte had a CE of only 99.4% and failed at around 200th cycle. In contrast, the asymmetrical cell in 2MP3 electrolyte manifest excellent cycling stability over 1000 cycles with an average CE of 99.9%. The Pr additive also affected the initial CE. As shown in Figure 2b, the initial CE in the 2 M electrolyte is 91.1%, which increases to 98.9% in the 50th cycle and 99.1% in the 200th cycle. In comparison, the CE in 2MP3 electrolyte at 1st, 50th, and 200th cycle is 98.5%, 99.5% and 99.8%, respectively, all of which are significantly greater than the CEs of 2 M electrolyte (Figure 2c). These results further confirm the positive effect of Pr additive in improving Zn reversibility.

Addition of Pr concomitantly tuned Zn deposition morphology and suppressed corrosion. As presented in Figure 2d, the cyclic voltammetry (CV) testing results indicated that Zn nucleation overpotential of Zn electrode in 2MP3 electrolyte is greater than that in 2 M electrolyte. The results are further confirmed by the voltage profiles of the initial Zn deposition
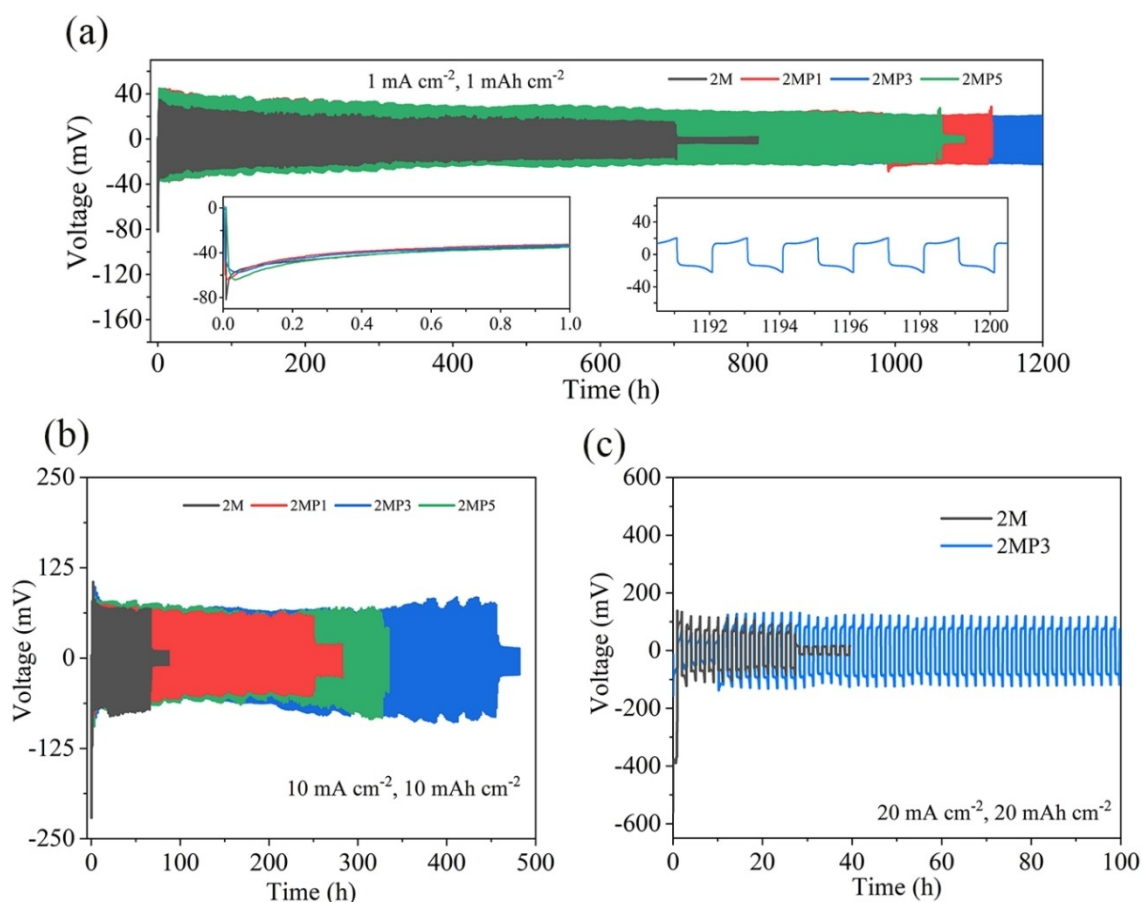

Figure 1. Cycling performance of Zn∥Zn symmetrical cells containing ZnSO$_4$ electrolytes with and without Pr additives at a) 1 mA cm^{-2}, 1 mAh cm^{-2}. b) 10 mA cm^{-2}, 10 mAh cm^{-2}. c) 20 mA cm^{-2}, 20 mAh cm^{-2}.

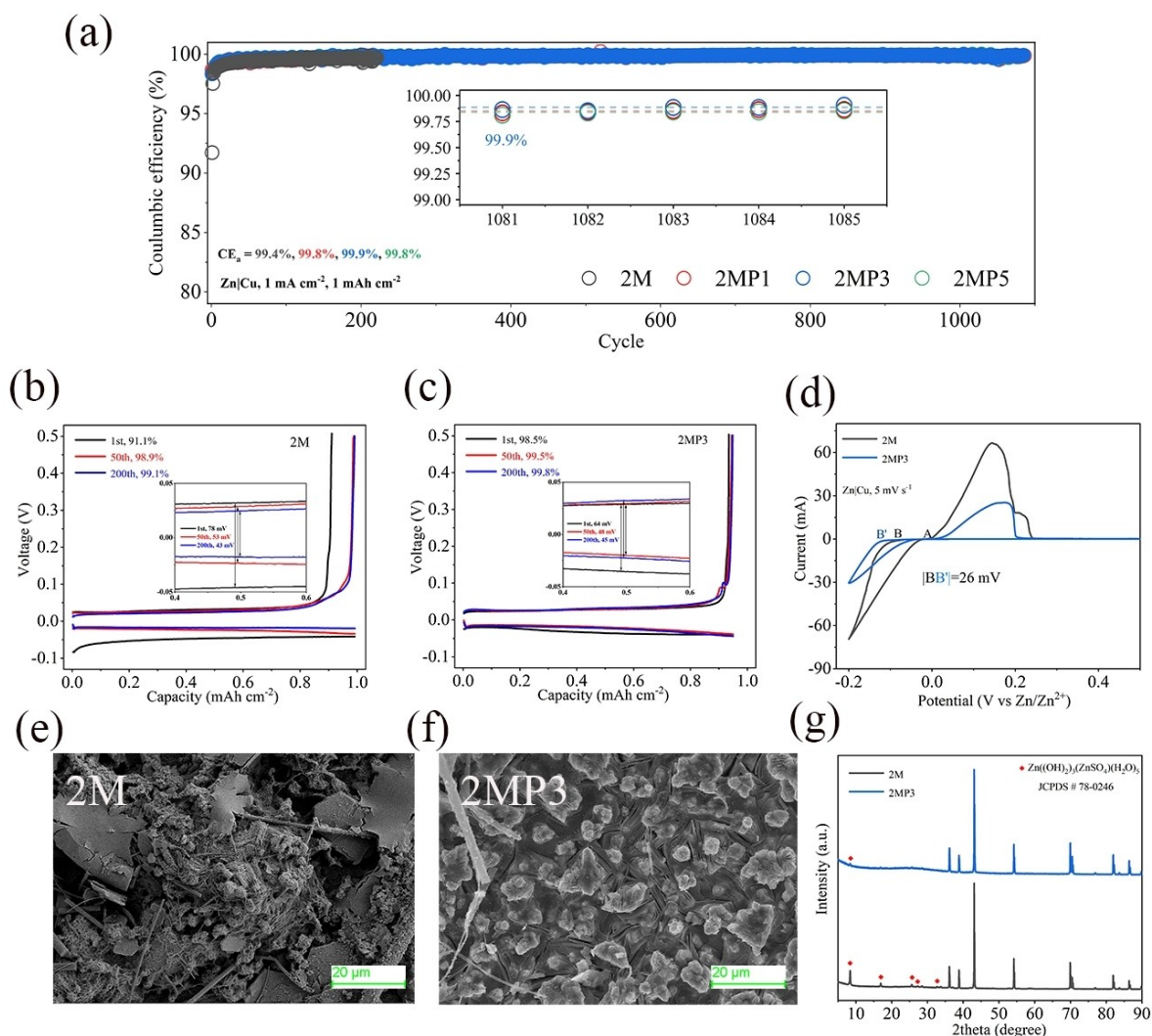**Figure 2.** Zn||Cu asymmetrical cell performance and properties. a) Coulombic efficiency (CE) of cells in different electrolytes at 1 mA cm^{-2},1 mAh cm^{-2}. b–c) Charge/discharge voltage profiles in b) 2 M and c) 2MP3 electrolyte at 1st, 50th and 200th cycle with magnified view of corresponding cycles in capacity range between 0.4 and 0.6 mAh cm^{-2} at current density 1 mA cm^{-2}. d) Cyclic voltammetry (CV) curves. SEM images of Zn electrode after 50 cycles in e) 2 M and f) 2MP3. g) XRD pattern of Zn electrode after 50 cycles.

(Figure S1, Supporting Information), suggesting a stronger driving force for the formation of finer Zn nuclei to inhibit random 2D diffusion and Zn dendrite formation.[26–27] The scanning electron microscopy (SEM) images confirmed that following 50 cycles with Zn||Cu cells, the Zn surface in the 2 M electrolyte become an apparent random and loose structure, Figure 2e, while there remained a densely integrated binding network structure on the Zn surface in the 2MP3 electrolyte, Figure 2f. XRD findings for the Zn electrode following cycling showed by-product $Zn((OH)_2)_3(ZnSO_4)(H_2O)_5$ in the 2 M electrolyte.[28–29] The peaks of byproduct however were significantly reduced in 2MP3 electrolyte (Figure 2g), confirming that Zn electrode corrosion was significantly suppressed. These findings were confirmed via a linear polarization test. As is seen in Figure 3a, the Zn corrosion voltage in 2MP3 electrolyte is −0.947 V, which is greater than that of pure $ZnSO_4$ electrolyte (−0.974 V). This finding evidences a lowered tendency for corrosion side reactions in 2MP3 electrolyte.[16] Linear sweep voltammetry (LSV) curves further confirm the positive impact of Pr additive (Figure S2, Supporting Information), where the oxygen evolution reaction (OER) overpotential increased and hydrogen evolution reaction (HER) potential negative shifted. The contact angle was characterized to understand the wettability of the electrolytes to Zn electrode. As presented in Figure 3b, a contact angle of 75° was measured in a 2 M electrolyte. However, the addition of Pr decreased the contact angle (70°), demonstrating that Pr molecules are likely to adsorb to the Zn surface compared to water, which is favorable for reducing the interfacial energy barriers and thus aids practically in a uniform electric distribution and production of homogeneous plating of Zn. The above results confirm the effectiveness of Pr to regulate the Zn deposition and suppress the corrosion.

To evaluate the effect of Pr additives on the properties of $ZnSO_4$ electrolyte, nuclear magnetic resonance (NMR), Raman and Fourier transform infrared spectroscopy (FT-IR) were

Batteries & Supercaps

Research Article
doi.org/10.1002/batt.202300526

Chemistry Europe
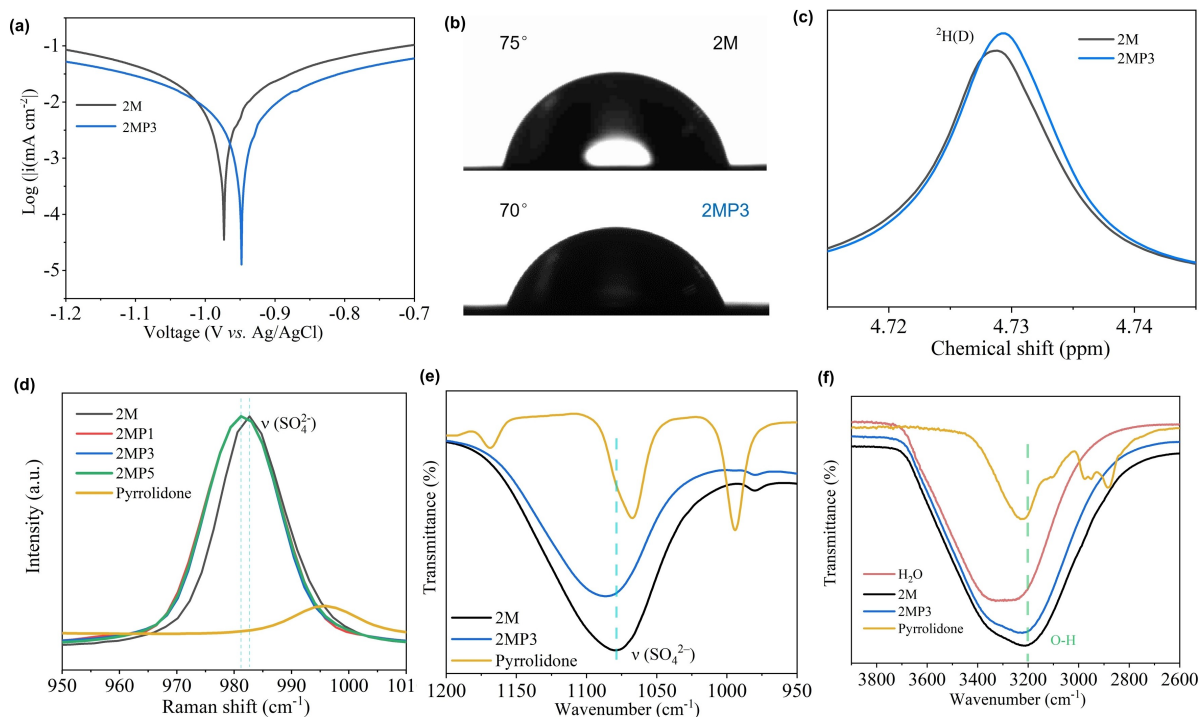European Chemical
Societies Publishing

Figure 3. Chemical and physical properties of electrolytes. a) Polarization of corrosion curves. b) Contact angle measurement of electrolytes with Zn-foil. c) ^{2}H NMR spectra for 2 M and 2MP3 electrolytes. d) Raman spectra in different electrolytes and Pr. e–f) FT-IR spectra in different electrolytes, Pr and H_2O.
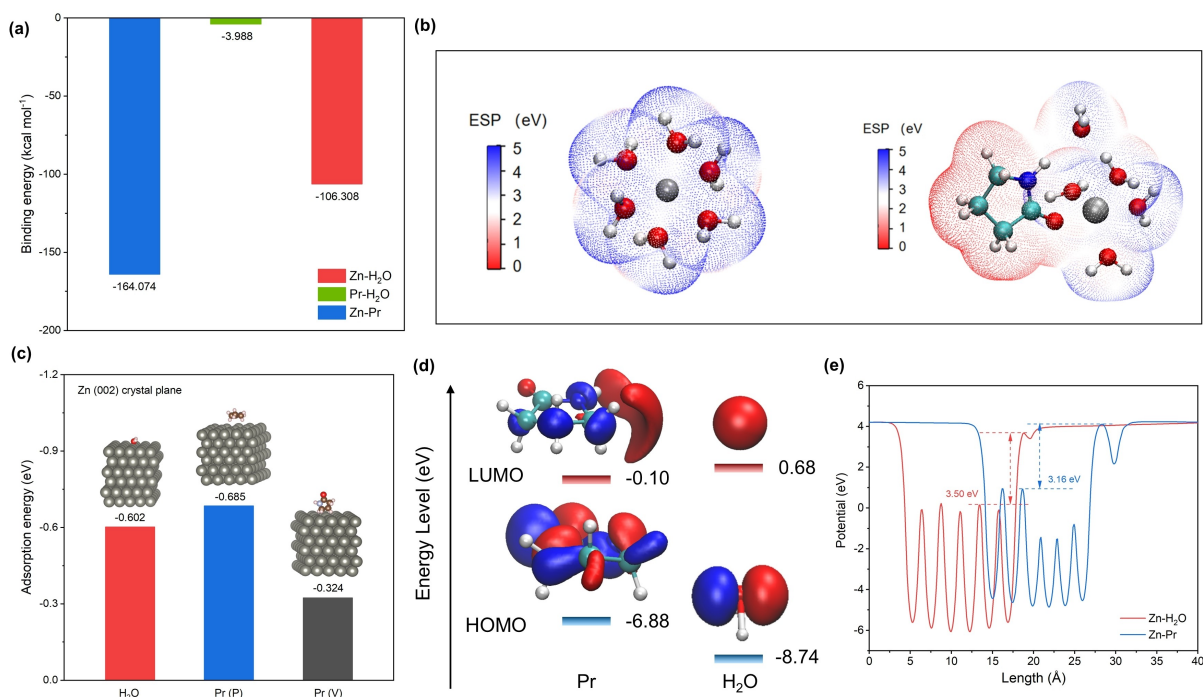

Figure 4. Theoretical computations. a) Binding energy of Zn–H_2O, Zn–Pr and Pr–H_2O. b) Electrostatic potential mapping of Zn^{2+}–$6H_2O$ (Left) and Zn^{2+}–$5H_2O$–Pr (Right) solvation structures. c) Adsorption energy of H_2O and Pr in Zn 002 crystal surface. d) LUMO and HOMO isosurfaces of Pr (Left) and H_2O (Right) molecules. e) Electrostatic potential distributions of Zn–Pr and Zn–H_2O.

characterized. As illustrated in Figure 3c, the ^{2}H peak locates at 4.728 ppm in the 2 M electrolyte, but the peak shifts after introducing 3% Pr, which is attributed to the decrease in surrounding electron density and the reduction in proton

shielding resulted from the interaction between Pr and D_2O molecules. The results indicate that the introduction of Pr into the electrolyte weakens the structure of the solvation inter-action of the Zn^{2+} and H_2O molecules.[19] This finding was
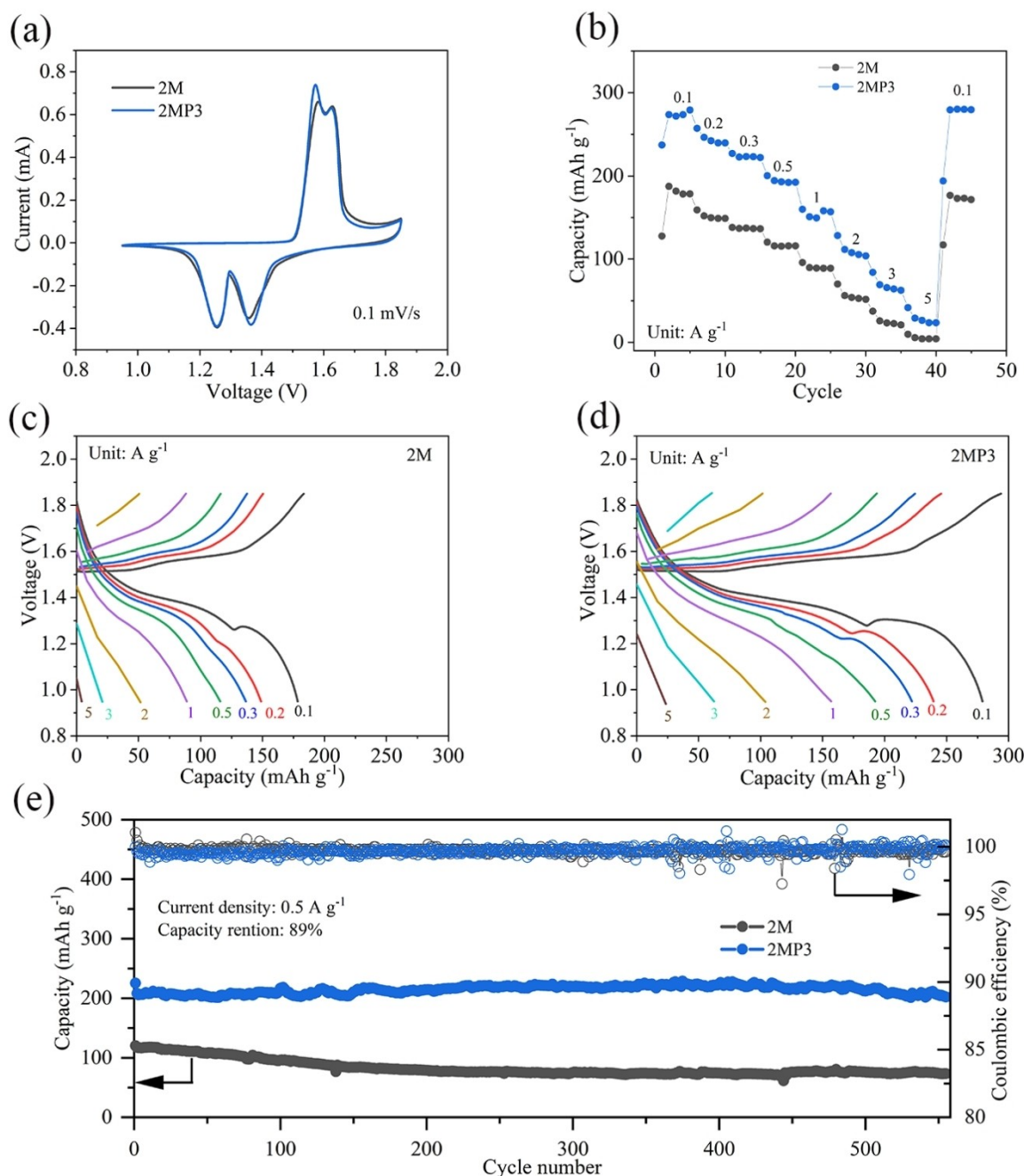
Batteries & Supercaps

Research Article
doi.org/10.1002/batt.202300526

Chemistry Europe
European Chemical
Societies Publishing

Figure 5. $Zn \| MnO_2$ full cell performance. a) Cyclic voltammetry (CV) curves. b) Rate performances at 0.1, 0.2, 0.3, 0.5, 1, 2, 3 and 5 $A\,g^{-1}$ in 2 M and 2MP3 electrolytes. c–d) Corresponding charge-discharge curves. e) Cycling performances at 0.5 $A\,g^{-1}$ in 2 M and 2MP3 electrolytes.

further verified by Raman and FT-IR spectra. The peak of SO_4^{2-} stretching vibration shifted with the addition of Pr (Figure 3d) and the O–H stretching vibration peak encountered a shift as well (Figure S3, Supporting Information). Furthermore, FT-IR spectra show the SO_4^{2-} stretching vibration peak at 1079.459 cm^{-1} in 2 M electrolyte and it has a blueshift (1086.691 cm^{-1}) after adding 3% Pr due to a weakened electrostatic coupling (Figure 3e). The O–H stretching vibration peak manifests a slight shift and peak intensity decreases in 2MP3 electrolyte (Figure 3f). The results demonstrated that the addition of Pr can affect the solvation structure.

The interaction amongst Zn^{2+} ion, H_2O, and Pr molecules was assessed via quantum chemistry computation. As presented in Figure 4a, the binding energy of Zn^{2+}–Pr was −164.074 $kcal\,mol^{-1}$, which was greater than that of Zn^{2+}–H_2O (−106.308 $kcal\,mol^{-1}$) and Pr–H_2O (−3.988 $kcal\,mol^{-1}$). It indicates that Pr molecules are more readily coordinated with Zn^{2+} than H_2O molecules. Furthermore, density functional theory (DFT) calculations were exploited to investigate interaction force among Zn^{2+}, Pr and H_2O. As depicted in Figure 4b, Pr molecule replaces a H_2O molecule in original solvation of Zn^{2+} −6H_2O, the regional value of the partial electrostatic potential

Batteries & Supercaps

Research Article
doi.org/10.1002/batt.202300526

Chemistry Europe
European Chemical
Societies Publishing

(ESP) decreases, resulting in a rapid transmission of Zn^{2+}. This is consistent with the mean-square displacement (MSD) results, where the diffusion coefficient of Zn^{2+} was increased with the introduction of Pr into the $ZnSO_4$ electrolyte (Figure S4, Supporting Information). Figure 4c compares the adsorption energy of Zn slab with Pr and H_2O molecules (perpendicular (Pr(V)) or parallel position (Pr(P)) along the Zn surface). The adsorption energy of Pr molecules with Zn (parallel to Zn plates Pr(P)) is greater than that of H_2O with Zn and Pr molecule with perpendicular state of Zn (Pr(V)). As a result, Pr molecules tend to adsorb parallel on the Zn surface, inhibiting 2D diffusion and facilitating uniform and compact Zn deposition as was seen in the SEM images. In addition, electron gain and loss of absorbed molecules on the Zn surface will impact the deposition behavior of zinc. As shown in Figure 4d, Pr has a smaller lowest unoccupied molecular orbital (LUMO) and a greater highest occupied molecular orbital (HOMO) than that for H_2O, indicating that electrons in Pr are more readily gained and lost when absorbing on the Zn surface. The results are further confirmed by the DFT calculation on the electrostatic potential distribution of Zn–H_2O and Zn–Pr, which reflects the difficulty of electron transfer from the Zn surface. The value of Zn–Pr is smaller than that of Zn–H_2O (3.16 eV vs. 3.50 eV), proving that electrons on Zn surface are more easily transferred to Pr (Figure 4e).

To assess the practical feasibility of Pr addition in boosting performance of the full cells, Zn||MnO_2 full cells were assembled. Cyclic voltammogram (CV) curves of the full batteries with and without Pr additive exhibited similar redox pairs, suggesting that Pr additive did not affect the redox reaction of cathode (Figure 5a). However, the rate performance of full batteries is significantly boosted (Figure 5b–d), resulting from the suppression of side reactions and the improved stability of Zn anode in 2MP3 electrolyte. The long-term cycling stability of full cells were assessed at 0.5 A g^{-1} (Figure 5e). Zn||MnO_2 full batteries in 2MP3 electrolyte exhibited a greater capacity of 201 mAh g^{-1} and capacity retention of 89% after 550 cycles than that in 2 M electrolyte (62% retention after 550 cycles). The boosted cycling performance in full batteries further confirms the positive effect of Pr additive.

Conclusions

A small amount of Pr additive was introduced into the conventional $ZnSO_4$ electrolyte to boost the reversibility and stability of the Zn electrode. Combined experiment, including, NMR, FT-IR, and Raman analysis, together with theoretical computation using MD and DFT confirmed that Pr additive regulates the solvation structure and alters the Zn anode–electrolyte interface via absorption on the Zn surface. This reduces the water activity and suppresses corrosion, by-product generation and Zn dendrite growth. The Zn electrode with 2MP3 electrolyte attained a high cycling reversibility process for over 1200 h at 1 mA cm^{-2} and 1 mAh cm^{-2}, delivered a high CE of 99.9% for 1000 cycle, and exhibited stable and reversible Zn plating/stripping cycling for over 100 h under harsh testing conditions of 20 mA cm^{-2} and 20 mAh cm^{-2}. The Zn||MnO_2 full cells with the Pr additive exhibited a high capacity of 201 mAh g^{-1} and good capacity retention of 89% after 550 cycles at 0.5 A g^{-1}.

Supporting Information

A file containing the supplementary information and details of the experiments and the theoretical calculation, and supplementary results figures (PDF). Additional references cited within the Supporting Information.[30–36]

Conflict of Interests

The authors declare no conflict of interest.

Data Availability Statement

The data that support the findings of this study are available from the corresponding author upon reasonable request.

Keywords: Zn electrode · Electrolyte additive · Solvation structure · Interface

[1] J. Wu, Y. Cao, H. Zhao, J. Mao, Z. Guo, *Carbon Energy* **2019**, *1*, 57–76.
[2] M. Li, C. Wang, K. Davey, J. Li, G. Li, S. Zhang, J. Mao, Z. Guo, *SmartMat* **2023**, *4*, e1185.
[3] S. Liu, R. Zhang, J. Mao, J. Yuwono, C. Wang, K. Davey, Z. Guo, *Appl. Phys. Rev.* **2023**, *10*, 021304.
[4] M. Song, H. Tan, D. Chao, H. J. Fan, *Adv. Funct. Mater.* **2018**, *28*, 1802564.
[5] G. Li, L. Sun, S. Zhang, C. Zhang, H. Jin, K. Davey, G. Liang, S. Liu, J. Mao, Z. Guo, *Adv. Funct. Mater.* **2023**, 2301291, DOI: 10.1002/adfm.202301291.
[6] B. Tang, L. Shan, S. Liang, J. Zhou, *Energy Environ. Sci.* **2019**, *12*, 3288–3304.
[7] J. Wan, R. Wang, Z. Liu, L. Zhang, F. Liang, T. Zhou, S. Zhang, L. Zhang, Q. Lu, C. Zhang, Z. Guo, *ACS Nano* **2023**, *17*, 1610–1621.
[8] Y. Geng, L. Pan, Z. Peng, Z. Sun, H. Lin, C. Mao, L. Wang, L. Dai, H. Liu, K. Pan, X. Wu, Q. Zhang, Z. He, *Energy Storage Mater.* **2022**, *51*, 733–755.
[9] Y. Chen, F. Gong, W. Deng, H. Zhang, X. Wang, *Energy Storage Mater.* **2023**, *58*, 20–29.
[10] D. Geng, Y. Tang, X. Han, Z. Cheng, L. Han, J. Liu, *Int. J. Electrochem. Sci.* **2023**, *18*, 100191.
[11] Q. Zhang, Y. Su, Z. Shi, X. Yang, J. Sun, *Small* **2022**, *18*, 2203583.
[12] F. Wang, O. Borodin, T. Gao, X. Fan, W. Sun, F. Han, A. Faraone, J. A. Dura, K. Xu, C. Wang, *Nat. Mater.* **2018**, *17*, 543–549.

[13] X. Lin, G. Zhou, M. J. Robson, J. Yu, S. C. T. Kwok, F. Ciucci, *Adv. Funct. Mater.* **2021**, *32*, 2109322.

[14] G. Li, Z. Zhao, S. Zhang, L. Sun, M. Li, J. A. Yuwono, J. Mao, J. Hao, J. Vongsvivut, L. Xing, C.-X. Zhao, Z. Guo, *Nat. Commun.* **2023**, *14*, 6526.

[15] S. Liu, J. Vongsvivut, Y. Wang, R. Zhang, F. Yang, S. Zhang, K. Davey, J. Mao, Z. Guo, *Angew. Chem. Int. Ed.* **2023**, *62*, e202215600.

[16] Y. Lyu, J. A. Yuwono, P. Wang, Y. Wang, F. Yang, S. Liu, S. Zhang, B. Wang, K. Davey, J. Mao, Z. Guo, *Angew. Chem. Int. Ed.* **2023**, *62*, e202303011.

[17] Z. Liu, R. Wang, Q. Ma, J. Wan, S. Zhang, L. Zhang, H. Li, Q. Luo, J. Wu, T. Zhou, J. Mao, L. Zhang, C. Zhang, Z. Guo, *Adv. Funct. Mater.* **2023**, 2214538.

[18] L. Cao, D. Li, T. Pollard, T. Deng, B. Zhang, C. Yang, L. Chen, J. Vatamanu, E. Hu, M. J. Hourwitz, L. Ma, M. Ding, Q. Li, S. Hou, K. Gaskell, J. T. Fourkas, X.-Q. Yang, K. Xu, O. Borodin, C. Wang, *Nat. Nanotechnol.* **2021**, *16*, 902–910.

[19] P. Sun, L. Ma, W. Zhou, M. Qiu, Z. Wang, D. Chao, W. Mai, *Angew. Chem. Int. Ed.* **2021**, *133*, 18395–18403.

[20] K. Zhu, C. Guo, W. Gong, Q. Xiao, Y. Yao, K. Davey, Q. Wang, J. Mao, P. Xue, Z. Guo, *Energy Environ. Sci.* **2023**, *16*, 3612–3622.

[21] Y. Wang, X. Zeng, H. Huang, D. Xie, J. Sun, J. Zhao, Y. Rui, J. Wang, J. A. Yuwono, J. Mao, *Small Methods* **2023**, 2300804.

[22] H. Huang, D. Xie, J. Zhao, P. Rao, W. M. Choi, K. Davey, J. Mao, *Adv. Energy Mater.* **2022**, *12*, 2202419.

[23] R. Li, M. Li, Y. Chao, J. Guo, G. Xu, B. Li, Z. Liu, C. Yang, Y. Yu, *Energy Storage Mater.* **2022**, *46*, 605–612.

[24] Y. Zhong, Z. Cheng, H. Zhang, J. Li, D. Liu, Y. Liao, J. Meng, Y. Shen, Y. Huang, *Nano Energy* **2022**, *98*, 107220.

[25] R. Wang, Q. Ma, L. Zhang, Z. Liu, J. Wan, J. Mao, H. Li, S. Zhang, J. Hao, L. Zhang, C. Zhang, *Adv. Energy Mater.* **2023**, *13*, 2302543.

[26] R. Qin, Y. Wang, M. Zhang, Y. Wang, S. Ding, A. Song, H. Yi, L. Yang, Y. Song, Y. Cui, J. Liu, Z. Wang, S. Li, Q. Zhao, F. Pan, *Nano Energy* **2021**, *80*, 105478.

[27] J. Li, Z. Guo, J. Wu, Z. Zheng, Z. Yu, F. She, L. Lai, H. Li, Y. Chen, L. Wei, *Adv. Energy Mater.* **2023**, *13*, 2301743.

[28] Y. Lin, Z. Mai, H. Liang, Y. Li, G. Yang, C. Wang, *Energy Environ. Sci.* **2023**, *16*, 687–697.

[29] Y. Lin, Y. Li, Z. Mai, G. Yang, C. Wang, *Adv. Energy Mater.* **2023**, *13*, 2301999.

[30] D. Xie, J. Zhao, Q. Jiang, H. Wang, H. Huang, P. Rao, J. Mao, *ChemPhysChem* **2022**, *23*, e202200106.

[31] M. J. Abraham, T. Murtola, R. Schulz, S. Páll, J. C. Smith, B. Hess, E. Lindahl, *SoftwareX* **2015**, *1 (2)*, 19–25.

[32] W. L. Jorgensen, J. Tirado-Rives, *PNAS* **2005**, *102*, 6665–6670.

[33] L. S. Dodda, J. Z. Vilseck, J. Tirado-Rives, W. L. Jorgensen, *J. Phys. Chem. B* **2017**, *121*, 3864–3870.

[34] G. Bussi, D. Donadio, M. Parrinello, *J. Chem. Phys.* **2007**, *126*, 014101.

[35] H. J. C. Berendsen, J. P. M. Postma, W. F. van Gunsteren, A. DiNola, J. R. Haak, *J. Chem. Phys.* **1984**, *81*, 3684–3690.

[36] M. M. Voronov, A. B. Pevtsov, S. A. Yakovlev, D. A. Kurdyukov, V. G. Golubev, *Phys. Rev. B* **2014**, *89*, 045302.